Thermodynamics and Reduction Kinetics Properties of 2-Methyl-3-hydroxypyridine-5-carboxylic Acid Oxygenase†

Pimchai Chaiyen, Pierre Brissette, David P. Ballou,* and Vincent Massey

Department of Biological Chemistry, University of Michigan, Ann Arbor, Michigan 48109-0606

Received September 16, 1996; Revised Manuscript Received November 25, 1996⊗

ABSTRACT: The investigation by absorbance and fluorescence rapid reaction spectrophotometry of the binding of the substrate MHPC (2-methyl-3-hydroxypyridine-5-carboxylic acid) or the substrate analog 5HN (5-hydroxynicotinic acid) to the flavoprotein MHPCO (2-methyl-3-hydroxypyridine-5-carboxylic acid oxygenase) shows that the binding proceeds in two steps. An enzyme−substrate complex initially formed is followed by a ligand-induced isomerization. This binding process is required for efficient reduction of the enzyme-bound flavin, as evidenced by the fact that MHPCO−substrate complexes can be reduced by NADH much faster than the enzyme alone. Since redox potential values of MHPCO and MHPCO−substrate complexes are the same, steric factors, such as the relative orientation of MHPC to the enzyme-bound flavin, are important for efficient hydride transfer to occur.

MHPCO[1] (EC 1.14.12.4) is an FAD-containing enzyme involved in the degradation of Vitamin B_6 (pyridoxine) by the soil bacterium, *Pseudomonas* MA-1 (Sparrow et al., 1969). Degradation of Vitamin B_6 proceeds via an oxidative pathway that is induced when these bacteria are grown on pyridoxine or pyridoxamine as their sole source of carbon and nitrogen (Burg et al., 1960; Sundaram & Snell, 1969). The pathway consists of a series of oxidative, hydrolytic, and decarboxylation reactions that convert pyridoxine to metabolites readily assimilated for growth. MHPCO catalyzes an oxygenation reaction and a ring cleavage of its substrate, MHPC, to yield AAMS, as shown in eq 1 (Sparrow et al., 1969).

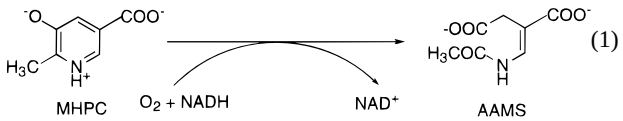

(1)

The reaction catalyzed by MHPCO is formally a dioxygenation, a reaction quite unusual for flavoenzymes (Massey & Hemmerich, 1975). Previous oxygen-18 tracer experiments with MHPCO (Sparrow et al., 1969) were inconclusive in establishing whether this enzyme incorporates one atom (monooxygenase) or both atoms (dioxygenase) of O_2 into the AAMS product. Nevertheless, MHPCO has been one of the two enzymes classified as flavoprotein dioxygenases (Sparrow et al., 1969; Hayaishi et al., 1975).

The biological cleavage of homocyclic and heterocyclic aromatic compounds is catalyzed largely by nonheme iron-containing dioxygenases (Hayaishi et al., 1975; Nozaki, 1974). Ferrous or ferric iron serves as the sole cofactor for these enzymes. In contrast, MHPCO only utilizes FAD and pyridine nucleotide cofactors and, in many respects, resembles the external flavoprotein monooxygenases, which require external reductants such as NADH or NADPH (Sparrow et al., 1969; Massey & Hemmerich, 1975; Kishore & Snell, 1981a−c). The catalytic cycle of MHPCO consists of two partial reactions (Kishore & Snell, 1981a): (a) a reductive half-reaction, in which the enzyme-bound FAD is reduced by pyridine nucleotide in a reaction that is greatly affected by the presence of MHPC, and (b) an oxidative half-reaction in which reoxidation of reduced FAD by molecular oxygen is accompanied by oxygenation and ring cleavage of the substrate. Conveniently, as is general with flavoprotein enzymes, this mechanism permits the reductive and oxidative phases of the reaction to be studied independently.

The work presented here focuses on the mechanism by which reduction of the enzyme-bound FAD is effected in MHPCO. Spectroscopic and rapid reaction kinetic studies examined the MHPCO-MHPC, and MHPCO-5HN (5-hydroxynicotinic acid, a substrate analog (Chaiyen et al., 1996)) complexes and the roles of the aromatic substrate and pyridine nucleotide in the reduction mechanism. The redox potentials of the MHPCO and the MHPCO−substrate complexes were also determined. Previous experiments with MHPCO demonstrated that MHPC accelerated the rate of enzyme reduction by pyridine nucleotide (Sparrow et al., 1969). This report confirms and quantifies this original observation and shows that binding of the substrate to the resting enzyme generates an activated enzyme−substrate complex that undergoes rapid reduction by pyridine nucleotide without significantly perturbing the redox potential of the enzyme-bound FAD. The reduction mechanism for MHPCO is very similar to mechanisms for the aromatic flavoprotein monooxygenases [see Massey and Hemmerich (1975), Ballou (1982), Entsch and Van Berkel (1995) for reviews)].

† This work was supported by the U.S. Public Health Service, GM 20877 (DPB) and GM 11106 (VM), and the Development and Promotion of Science and Technology Talent Project, Thailand (PC).

* To whom correspondence should be addressed.

⊗ Abstract published in *Advance ACS Abstracts,* February 1, 1997.

[1] Abbreviations: MHPC, 2-methyl-3-hydroxypyridine-5-carboxylic acid; MHPCO, 2-methyl-3-hydroxypyridine-5-carboxylic acid oxygenase; 5HN, 5-hydroxynicotinic acid; AAMS, α-(*N*-acetylamino-methylene)succinic acid; E_{ox}, and E_{red}, oxidized and reduced forms of MHPC oxygenase; DTT, dithiothreitol; ITS, indigo trisulfonate; MOPS, 3-[*N*-morpholino]propanesulfonic acid; NADH, *β*-nicotinamide adenine dinucleotide reduced form; 4R-NADD; 4-(*R*)-^{2}H-*β*-nicotinamide adenine dinucleotide reduced form.

S0006-2960(96)02325-2 CCC: $14.00

MATERIALS AND METHODS

Reagents. Pyridoxine hydrochloride, NAD^+, NADH, alchohol dehydrogenase, d_5-ethanol, DEAE-sepharose (fast flow), and Phenyl-sepharose were from Sigma Chemical Co. Sodium dithionite was from J. T. Baker Chemical Co. Hydroxyapatite Bio-Gel HT was from Biorad. Pyridoxine, diazald, nitrobenzene, and HBr were from Aldrich Chemical Co. 5-Hydroxynicotinic acid methyl ester was from TCI Chemical Co. Silica gel was from EM science. 4R-NADD was prepared following a procedure described by Loesche et al. (1980) and Gassner et al. (1994). The concentrations of the following compounds were determined using known extinction coefficients at pH 7.0: NADH and NADPH, $\epsilon_{340} = 6.22\ mM^{-1}\ cm^{-1}$ (Horecker & Kornberg, 1948); MHPC, $\epsilon_{326} = 4.4\ mM^{-1}\ cm^{-1}$ (Kishore & Snell, 1979). 5HN has an extinction coefficient of $4.19\ mM^{-1}\ cm^{-1}$ (0.1 N NaOH) at 315 nm. The concentration of the purified enzyme was measured using the previously determined molar absorption coefficient of $13\ 110\ M^{-1}\ cm^{-1}$ at 454 nm (Kishore & Snell, 1981b).

Spectroscopic Studies. UV−visible absorbance spectra were recorded with a Hewlett-Packard diode array spectrophotometer (HP 8452A) or a Cary model 3E double-beam spectrophotometer. Single-wavelength enzymatic assays were conducted with a Cary model 219 double-beam spectrophotometer. All spectrophotometers were equipped with thermostated cell compartments. Fluorescence spectra were recorded with a ratio spectrofluorometer designed and built by Dr. David P. Ballou and Mr. Gordon Ford of the University of Michigan. ^{1}H NMR spectra were recorded with a General Electric GN500, 500 MHz NMR instrument. Chemical shift values are reported in parts per million relative to tetramethyl silane.

MHPC. This compound was prepared as described previously (Palm et al., 1967) with the following modifications. After completion of the methylation of pyridoxine to 3-*O*-methylpyridoxine, the reaction mixture was not treated as in Stiller et al. (1939) but was dissolved in a small amount of methanol. Silica gel (60H) (20 g) was added into the crude solution. The mixture was then evaporated to remove methanol, and the sample was applied to a (silica gel) column (3.0×40 cm) pre-equilibrated with chloroform. The column was then washed with 800 mL of chloroform:methanol (95:5). 3-*O*-methyl pyridoxine was eluted after 270 mL of the eluent had washed through the column. This compound has an $R_f = 0.41$ on silica (Polygram Sil G/UV 254) thin-layer chromatography with chloroform:methanol (90:10) as the solvent. The desired fractions of 3-*O*-methylpyridoxine were pooled and solvent was removed with a rotary evaporator (yield was 52%). The compound has a melting point of 104−105.5 °C and a λ_{max} (0.1 N NaOH) at 276 nm. ^{1}H NMR spectrum: (d_6-acetone) δ 2.48 (3H, s, CH_3), 3.8 (3H, s, OCH_3), 4.69 (2H, s, CH_2OH), 4.79 (2H, s, CH_2OH), 8.01 (1H, s, ArH).

3-*O*-Methylpyridoxine was then oxidized to 2-methyl-3-methoxypyridine-4,5-dicarboxylic acid according to the Palm et al. (1967) procedure. After completion of the reaction, the material was chromatographed on a Dowex-1 formate column as described. Fractions containing 2-methyl-3-methoxypyridine-4,5-dicarboxylic acid were analyzed by UV−visible spectroscopy. The product has a λ_{max} of 286 nm in acid solution. These fractions were pooled and evaporated to dryness. The compound was then crystallized from hot water (yield of the crystalline product was 46%). ^{1}H NMR spectrum: (d_6-DMSO) δ 2.48 (3H, s, CH_3), 3.73 (3H, s, OCH_3), 8.7 (1H, s, ArH).

2-Methyl-3-methoxypyridine-4,5-dicarboxylic acid was decarboxylated to 2-methyl-3-methoxypyridine-5-carboxylic acid according to the Palm et al. (1967) procedure. The crude mixture was washed with ether, dissolved in water, and applied to a Sep-Pak C_{18} cartridge (prewashed with water and methanol). The cartridge was eluted with water several times. The eluate containing the product was evaporated to yield a white solid with recovery of the dried product at 95%. The compound has an $R_f = 0.55$ on silica thin-layer chromatography with chloroform:methanol (90:10) and a few drops of acetic acid as solvent. ^{1}H NMR spectrum: (d_6-DMSO) δ 2.39 (3H, s, CH_3), 3.85 (3H, s, OCH_3), 7.62 (1H, s, ArH), 8.51 (1H, s, ArH).

2-Methyl-3-hydroxypyridine-5-carboxylic acid was obtained by demethylation of 2-methyl-3-methoxypyridine-5-carboxylic acid. Complete conversion to the 3-hydroxy derivative was attained after 13 h of gentle refluxing in 48% HBr, compared to a suggested 4 h by Palm et al. (1967). The reaction mixture was then evaporated to dryness under reduced pressure. The residue was extracted with dichloromethane to remove an orange-colored contaminant, and the product was collected on a filter and dried (yield was 82%). The compound has an $R_f = 0.22$ on silica thin-layer chromatography with chloroform:methanol (90:10) and a few drops of acetic acid as solvent. ^{1}H NMR spectrum: (d_6-DMSO) δ 2.35 (3H, s, CH_3), 7.87 (1H, s, ArH), 8.43 (1H, s, ArH).

5HN. 5-Hydroxynicotinic acid methyl ester was stirred in 10 N NaOH at room temperature for 3 h. The product solution was acidified to pH 1.1 with 6 N HCl. The resulting white precipitate was washed several times with ice-cold water. The compound has an $R_f = 0.28$ on silica thin-layer chromatography with chloroform:methanol (90:10) and a few drops of acetic acid as solvent. λ_{max} (0.1 N NaOH) = 315 nm; λ_{max} (0.1 N HCl) = 290 nm. ^{1}H NMR spectrum: (d_6-DMSO) δ 7.76 (1H, s, ArH), 8.11 (1H, s, ArH), 8.39 (1H, s, ArH).

Growth of Organisms. *Pseudomonas* MA-1 was a generous gift from Dr. Esmond E. Snell, Departments of Microbiology and Chemistry, The University of Texas (Austin, TX 78712). This bacterial strain has been deposited with the American Type Culture Collection (ATCC 33286). Bacteria were grown in minimal medium B containing casein hydrolysate (0.1 g/L) and supplemented with pyridoxine as its major carbon and nitrogen source (Guirard & Snell, 1971). The pH of the medium was adjusted to 7.0. A solution of pyridoxine (0.1 g/mL in 50 mM sodium phosphate buffer, pH 7.0), supplemented with a complete vitamin mixture, was sterilized by filtration and added aseptically to previously autoclaved medium B to provide 0.2 g of pyridoxine per 100 mL of growth medium (Guirard & Snell, 1971). Large-scale cultures were grown at 28−30 °C in a 250 L New Brunswick fermentor (aeration at 150 L/min) from a 2−2.5% inoculum. Cells were harvested in early stationary phase in a Sharples centrifuge and stored in liquid nitrogen until used.

Long-term preservation of the stock culture of *Pseudomonas* MA-1 was effected by storage of the culture at −85 °C in the presence of glycerol. The culture is maintained in a sterile mineral salts medium containing glycerol. This

medium is a 0.1 M sodium/potassium phosphate buffer at pH 7.0 containing the following salts per 100 mL of medium: NH_4Cl, 0.2 g; $FeSO_4 \cdot 7\ H_2O$ (0.1% solution), 0.05 mL; $MgSO_4$, 0.01 g; $CaCl_2$ (1% solution), 0.1 mL. The $CaCl_2$ solution was sterilized separately and added to a previously sterilized medium. The culture to be stored was freshly grown on a nutrient plate of medium B containing 0.2% pyridoxine. Bacterial growth from the plate was scraped into a sterile tube containing 0.75 mL of mineral salts medium, and the tube was stirred to resuspend the cell paste. The contents of this tube were poured into a sterile screw-capped tube containing 1.0 mL of sterile reagent grade glycerol. The contents of this tube were thoroughly mixed and the tightly capped tube was stored at −85 °C.

Assay for MHPCO. MHPCO was assayed by monitoring the disappearance of MHPC and NADH at 340 nm as described by Sparrow et al. (1969). The decrease in absorbance at 340 nm results from consumption of both MHPC ($\epsilon = 2.39 \times 10^3\ M^{-1}\ cm^{-1}$) and NADH ($\epsilon = 6.22 \times 10^3\ M^{-1}\ cm^{-1}$). One unit of activity is defined as the oxygenation of 1 μmol of MHPC per min at 25 °C, which corresponds to a decrease in absorbance of 8.6 per min at 340 nm of a reaction mixture in 1 mL.

Purification of MHPCO. The purification scheme described previously (Sparrow et al., 1969) was modified to include additional steps. Buffers used for enzyme purification contained 0.3 mM EDTA and 1 mM DTT unless otherwise specified. All operations were carried out at 4−5 °C.

Step 1: Preparation of Crude Extract. Frozen cell paste of *Pseudomonas* MA-1 (150 g) in 200 mL of 100 mM sodium phosphate buffer, pH 8.0, containing 5 mM EDTA, 5 mM DTT, and 57 μM phenylmethylsulfonyl fluoride was thawed for 9−10 h at 4 °C and the cells were resuspended by stirring with a glass rod. The cells were disrupted by sonic treatment using a Branson Model 250 sonifier for a total sonication time of 20 min. The temperature of the suspension was maintained below 15 °C during sonication. The suspension was then centrifuged (16000*g*) for 30 min and the supernatant was saved. The pelleted cells were resuspended in 200 mL of extraction buffer, sonicated and centrifuged as described before, and the supernatant solution was decanted. The supernatants were combined and centrifuged (100000*g*) for 1 h to produce a supernatant defined as the crude extract. Oxygenase activity in the crude extract was determined by subtracting the basal NADH oxidase activity (assay mixture minus MHPC) from the total activity measured in the presence of MHPC. The MHPC-independent NADH oxidase activity of the crude extract is resolved from the oxygenase activity in step 3 of the purification procedure. Substitution of NADH in the enzyme assay by NADPH lessens, but does not eliminate the oxidase activity in the crude extract.

Step 2: Nucleic Acid Removal. To the crude extract was added dropwise a 1% (w/v) solution of protamine sulfate freshly prepared in 20 mM sodium phosphate, pH 8.0, to a final level of 2.8 mg/g of cell paste used in step 1. The resulting suspension was stirred for an additional 15 min and was centrifuged (16000*g*) for 30 min.

Step 3: Ammonium Sulfate Fractionation. The supernatant solution was then subjected to a 0−40% ammonium sulfate fractionation. The pH of the suspension was maintained at 8.0 with ammonium hydroxide during addition of solid ammonium sulfate. The suspension was stirred for an additional 20 min and centrifuged as before. The pellet contained the NADH oxidase activity and was discarded. Additional ammonium sulfate (to 80% saturation) was added to the oxygenase supernatant and the suspension was centrifuged (100000*g*) for 90 min. The pellet was redissolved in 30 mM triethanolamine buffer (pH 7.5) and was dialyzed against 20 L of this triethanolamine buffer for 8 h.

Step 4: DEAE-Sepharose Chromatography. The dialyzed enzyme from step 3 was applied to a DEAE-Sepharose column (2.8 × 22 cm) equilibrated with 30 mM triethanolamine buffer, pH 7.5, and washed with 400 mL of the buffer. Protein was eluted with a 1 L gradient of 0−200 mM NaCl in the triethanolamine buffer. Fractions were pooled according to their oxygenase activity and their UV−visible spectra. The enzyme solution was concentrated and dialyzed against 4 L of 10 mM sodium phosphate buffer, pH 6.8.

Step 5: Hydroxyapatite Chromatography. The dialyzed material from above was applied to an hydroxyapatite column (Bio-gel HT, Biorad) (2.8 × 22 cm) that was equilibrated with 10 mM sodium phosphate buffer, pH 6.8. A 1 L linear gradient of 10−150 mM sodium phosphate buffer, pH 6.8, was applied to elute the proteins. The active yellow fractions were pooled and, in the presence of about 20 μM added FAD, concentrated using an Amicon PM-30 ultrafiltration membrane. To the concentrated enzyme was added a saturated ammonium sulfate solution, pH 7.8, to make a final ammonium sulfate saturation of 25%.

Step 6: Phenyl-Sepharose Chromatography. The sample from step 5 was applied to a phenyl-Sepharose column (1.7 × 15 cm) pre-equilibrated with 30 mM sodium phosphate buffer containing ammonium sulfate (25% saturation), pH 6.8. The column was washed with 50 mL of this buffer. Elution of the protein was effected with a 500 mL combination linear gradient of ammonium sulfate (25 to 0%) and ethylene glycol (0 to 25% v/v) in 30 mM sodium phosphate buffer (pH 6.8) and 10 μM FAD. After the gradient, elution was continued with 100 mL of sodium phosphate buffer containing 25% (v/v) ethylene glycol, pH 6.8. Active fractions were pooled and concentrated with a Centriprep concentrator (PM-30) in the presence of 20 μM FAD. The concentrated enzyme was equilibrated in 50 mM MOPS, pH 6.8, 0.3 mM EDTA, 1 mM DTT buffer by passage through a Sephadex G-25 column in this buffer. The enzyme, approximately 80 μM, was frozen as 200 μL aliquots in a dry ice−isopropanol bath and stored at −85 °C.

This procedure results in the efficient purification of MHPCO to approximately 90% homogeneity as judged by SDS−PAGE. A yield of 50−60 mg of protein with a specific activity of 4.03 units/mg was isolated from 150 g of cell paste. The primary difference between this purification and that published by Sparrow et al. (1969) is the introduction of phenyl-Sepharose and DEAE-Sepharose chromatography steps and the elimination of the crystallization step. The spectral characteristics of the enzyme are identical to those of crystalline MHPCO reported by Kishore and Snell (1981b). The purification results of MHPCO are summarized as in Table 1.

Enzyme Activation. Upon storage at 0−4 °C, the enzyme slowly inactivates. The inactive enzyme has FAD bound that can be reduced slowly by NADH in the presence of the substrate. The conversion between the inactive and active enzyme is reversible and can be effected by incubating with

Table 1: Purification Table

purification step	activity (unit)	yield (%)	specific activity (unit/mg)	fold of purification
crude	701	100	0.079	1
protamine sulfate	647	92	0.074	1
40% NH_4SO_4 fractionation	638	91	0.121	1.5
DEAE-Sepharose	380	54	3.25	41
hydroxyapatite	287	41	3.46	44
phenyl-Sepharose	222	32	4.03	51

10 mM DTT, 100 μM FAD at 25 °C for 1 h. The activated enzyme is then passed through a Sephadex G-25 column equilibrated with the appropriate buffer in order to remove excess FAD and used within 1−2 days.

Rapid Reaction Experiments. Rapid kinetic measurements were performed with a Hi-Tech Scientific Model SF-61 stopped-flow spectrophotometer that was controlled by a Macintosh IIcx using KISS software (Kinetic Instruments, Inc.). The optical path length of the observation cell is 1 cm. The stopped-flow apparatus was made anaerobic by flushing the flow system with an anaerobic buffer solution consisting of 0.1 unit/mL of protocatechuic acid dioxygenase (Bull & Ballou, 1981) and 400 μM protocatechuic acid. This solution was allowed to stand in the flow system overnight. The flow unit was then thoroughly rinsed with anaerobic buffer before experiments. Data analysis and simulation were carried out using program A (developed by Chung-Jen Chiu, Rong Chang, Joel Dinverno, and Dr. David Ballou, University of Michigan), which permits the analysis of experimental data by exponential fits based on the Marquardt algorithm (Press et al., 1992). The graphical determinations of rate constants used a Levenberg−Marquardt nonlinear fit algorithm that is included in the KaleidaGraph software (Synergy Software, Reading, PA).

Catalytic Reductions. Reductions of E_{ox} and E_{ox}−substrate complexes were carried out by using xanthine and xanthine oxidase as a reduction system (Massey, 1991). Briefly, a solution of MHPCO, xanthine, benzyl viologen, and xanthine oxidase (side arm) in a specially designed cuvette equipped with two side arms and a stopcock was made anaerobic by repeated cycles of evacuation and flushing with oxygen-free argon. After anaerobiosis had been established, the reduction was initiated by adding xanthine oxidase from a side arm. The reduction was monitored by recording spectra with a Hewlett-Packard diode array spectrophotometer.

Redox Potential Determination. MHPCO and indigo trisulfonate (ITS) (side arm) were made anaerobic as described above. The reduction was begun by mixing the dye from the side arm with MHPCO in the main body of the cuvette. The MHPCO and ITS were slowly reduced by DTT in the buffer solution. The reduction of enzyme was monitored at 490 nm, the isobestic point for ITS and ITS reduction was monitored at 602 nm, where flavin does not have absorbance. The ratio of oxidized and reduced species of MHPCO and ITS was calculated. The midpoint potential (E_m) can be calculated using the standard Nernst equation. The value of −0.081 V was used for the midpoint potential value of ITS.

RESULTS

Reductions of E_{ox} and E_{ox}−Substrate Complexes. Although NADH is the physiological reductant of the enzyme-bound FAD, MHPCO can also be reduced by the xanthine−xanthine oxidase reduction system (Massey, 1991) by sodium dithionite, photochemical reduction, or sodium borohydride (Sparrow et al., 1969). Figure 1A shows representative spectra obtained during the anaerobic reduction of MHPCO with the xanthine−xanthine oxidase reduction system. The intermediate species observed in the conversion of oxidized to reduced enzyme has an absorbance spectrum characteristic of a red anionic flavin semiquinone (Massey & Palmer, 1966). The maximum amount of anionic semiquinone kinetically observed at half-reduction under these conditions was estimated to be 81% from a plot of the absorbance at 520 nm versus the absorbance at 484 nm (inset of Figure 1A). A similar amount of semiquinone was also observed during titrations using sodium dithionite as a reductant. The amount of anionic semiquinone at equilibrium was quantified by stopping the xanthine−xanthine oxidase reduction system, when anionic semiquinone was formed at 81%, by adding

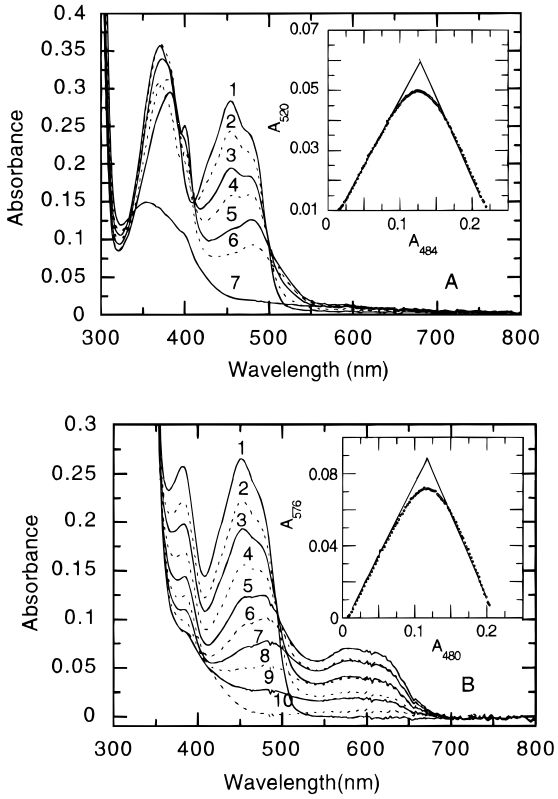

FIGURE 1: (A) Reduction of MHPCO with the xanthine−xanthine oxidase system. Enzyme (20.7 μM) in 50 mM sodium phosphate buffer, pH 7.0, 1 mM DTT, 0.3 mM EDTA, 25 °C was catalytically reduced by xanthine (400 μM), xanthine oxidase (20 nM), and benzyl viologen (5 μM) in an anaerobic cuvette. The reaction was monitored spectrally: 1, oxidized enzyme; 2, 27; 3, 51; 4, 71; 5, 101; 6, 131 min after reduction had begun; and 7, reduced enzyme. The inset to the figure shows the plot of the absorbance at 520 nm versus the absorbance at 484 nm. The solid line represents the extrapolation to 100% of red semiquinone. (B) Reductive titration of MHPCO−MHPC complex with the xanthine−xanthine oxidase system. Enzyme (19.6 μM) plus 300 μM MHPC in 50 mM sodium phosphate buffer, pH 7.0, 1 mM DTT, 0.3 mM EDTA, 25 °C was catalytically reduced by xanthine (400 μM), xanthine oxidase (20 nM), and benzyl viologen (5 μM) in an anaerobic cuvette. The reaction was monitored spectrally: 1, oxidized enzyme; 2, 17; 3, 32; 4, 52; 5, 72; 6, 92; 7, 112; 8, 132; 9, 152 min after reduction had begun; and 10 reduced enzyme. The inset figure shows the plot of the absorbance at 576 nm versus the absorbance at 480 nm. The solid line represents the extrapolation to 100% of blue semiquinone.

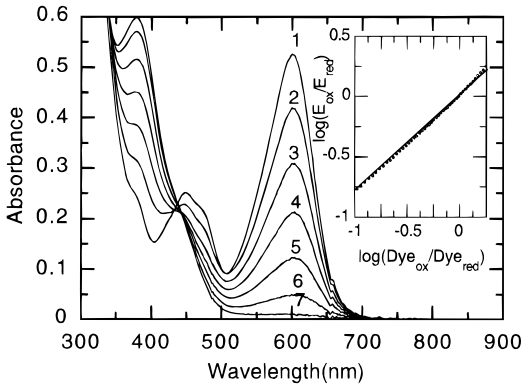

FIGURE 2: Determination of the redox potential of the MHPCO−5HN complex. Enzyme (15.6 μM), 5HN (200 μM), and ITS (20 μM) in 50 mM sodium phosphate, pH 7.0, 0.3 mM EDTA, 0.15 mM DTT, 25 °C, was slowly reduced by DTT in the buffer solution in an anaerobic cuvette. The reaction was followed spectrally: 1, oxidized enzyme and dye; 2, 20; 3, 50; 4, 80; 5, 110; 6, 140 min after reduction began; and 7 reduced enzyme and dye. Inset: The reduction of ITS was monitored by the decrease in absorbance at 602 nm, and the reduction of the enzyme was monitored by the decrease in absorbance at 490 nm, allowing the ratio of oxidized and reduced species to be calculated. The slope of the linear part of the plot of $\log(E_{ox}/E_{red})$ and $\log(Dye_{ox}/Dye_{red})$ was 0.8.

oxypurinol (200 μM), a potent xanthine oxidase inhibitor (Massey et al., 1970). After adding this inhibitor, approximately 61% of the semiquinone slowly disproportionated to E_{ox} and E_{red} over a period of 1 day, indicating that at equilibrium about 20% of anionic semiquinone exists in solution.

When MHPCO was reduced with the xanthine−xanthine oxidase system in the presence of MHPC (the natural substrate), an intermediate species with long-wavelength absorbance is observed as shown in Figure 1B. A similar long-wavelength intermediate species is also observed when 5HN (the substrate analog) (Chaiyen et al., 1996) is used instead of MHPC (data not shown). These spectra have the characteristics of blue neutral flavin semiquinones (Massey & Palmer, 1966). A plot of the absorbance at 576 nm versus the absorbance at 480 nm indicated that under the conditions of Figure 1B the neutral semiquinone species formed with a yield of 83% for the MHPCO−MHPC complex (inset of Figure 1B); a similar experiment indicated that the neutral semiquinone formed with a yield of 84% for MHPCO−5HN complex (data not shown). Extrapolation of the linear portion of the plots to 100% semiquinone formation indicated that the extinction coefficient at 576 nm for the MHPCO−MHPC complex was 4440 M^{-1} cm^{-1}, while the extinction coefficient at 570 nm for the MHPCO−5HN complex was 4350 M^{-1} cm^{-1}. These values fall within the range observed experimentally with other flavoprotein semiquinones (3000−5000 M^{-1} cm^{-1}) (Massey & Palmer, 1966). We used oxypurinol (200 μM) to stop the xanthine−xanthine oxidase reaction at the maximum point of semiquinone formation and followed the ensuing disproportionation reaction of the quasi-stable semiquinone species. It was estimated that at equilibrium about 13 and 34% of neutral semiquinone remained in solution for the MHPCO−MHPC and MHPCO−5HN complexes, respectively.

Redox Potential Determinations. The redox potentials of the free enzyme and of its complexes with MHPC and 5HN (Figure 2) were determined by using ITS as the standard dye and DTT as reductant as described in Materials and Methods. We were interested in determining the two-electron reduction potential, since that is relevant for the reactions with NADH. We cannot use the xanthine−xanthine oxidase system as reductant, since this system forms the quasi-stable semiquinone, which makes the analysis complicated. We have found that DTT, which is required in the buffer solution for MHPCO activity (Sparrow et al., 1969; Kishore & Snell, 1981a), can be used as a two-electron reductant for MHPCO in the presence of dye. During the reduction process ITS was reduced by DTT via a two-electron reduction process. Reduced ITS then reduced the enzyme. Since the process involves the transfer of two electrons, no significant amount of semiquinone was observed. Thus, the midpoint potential ($E_m°$) obtained from the plots of log (E_{ox}/E_{red}) and log (dye_{ox}/dye_{red}) is that of the oxidized enzyme/reduced enzyme couple (inset of Figure 2). This is supported by the fact that the slopes of these plots are close to unity. A small deviation from linearity at the beginning of the plots may be due to insufficient equilibration between ITS and enzyme at early stages of the reduction. Therefore, this part of the plot was not used in the calculation of the redox potentials. Using the linear portions of the data, individual experiments yielded $E°'$ values with a precision of ±3 mV. Using all of the data, including the nonlinear portion, fits for the values for $E°'$ decreased by 4 mV or less. The redox potential of the uncomplexed enzyme, enzyme−MHPC, and enzyme−5HN was determined to be −85, −78, and −81 mV, respectively. We consider these values to be essentially the same within our experimental uncertainty.

Table 2: Redox Potential Values

	E_m (mV)	$E_1°'$ (mV)	$E_2°'$ (mV)	% semiquinone at equilibrium
enzyme	−85	−102	−68	20
enzyme-MHPC	−78	−108	−48	13
enzyme-5HN	−81	−80	−82	34

Since the maximum amount of semiquinone stabilized is estimated from the experiments that did not include ITS, we can use eqs 2 and 3 (Clark, 1960; Einarsdottir et al., 1988) to estimate the potentials of the individual electron transfer steps. Where M = the maximum fraction of thermodynamically stable semiquinone formed, $T = 298$, E_m = the two-electron reduction potential, E_1' = the oxidized enzyme/semiquinone half potential, and E_2' = the semiquinone/reduced enzyme half potential. E_m, E_1', and E_2' values of the enzyme and its complexes are listed in Table 2.

$$E_1°' - E_2°' = 2(2.303RT/F)\log[2M/(1 - M)] \quad (2)$$

$$E_1°' + E_2°' = 2E_m \quad (3)$$

Kinetics of the Binding of MHPC to Oxidized MHPCO (E_{ox}). The mechanism of interaction between E_{ox} and MHPC was studied by stopped-flow fluorimetry. A solution of uncomplexed MHPCO was mixed with solutions containing various concentrations of MHPC. The change in enzyme-bound FAD fluorescence was monitored by using an excitation wavelength of 468 nm with observation of all emission intensity above 515 nm. The binding of MHPC to the E_{ox} results in an increase of flavin fluorescence (Figure 3). The apparent rate constant for the formation of the complex approaches a limiting value at high MHPC concentrations

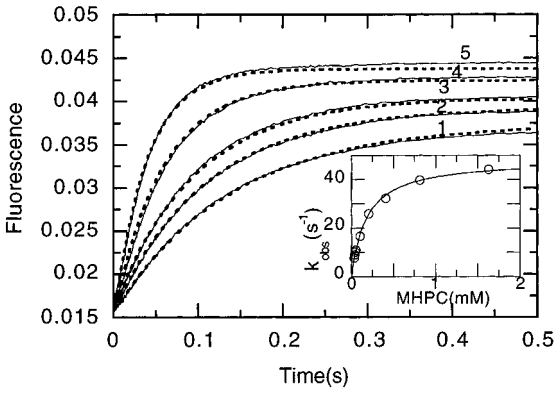

FIGURE 3: Binding of MHPC to the enzyme. (Solid line) enzyme (8.5 μM) was mixed with different concentrations of MHPC: 1, 58.4; 2, 81; 3, 99; 4, 197.8; and 5, 401.4 μM in 50 mM sodium phosphate buffer, pH 7.0, 1 mM DTT, 4 °C. The reaction was monitored with stopped-flow fluorescence with an excitation wavelength of 468 nm and emission wavelengths greater than 515 nm. The simulated data of each concentration of MHPC according to the model and rate constants in Scheme 3 and Table 2 are shown as dotted lines. The inset to the figure shows graphical determination of the kinetic parameters for the binding of MHPC to the enzyme. Observed rate constants (k_{obs}) of the fluorescence change when MHPC was mixed with the enzyme are plotted versus MHPC concentration (after mixing).

Scheme 1

$$E_{ox} + S \underset{k_2}{\overset{k_1}{\rightleftharpoons}} E_{ox}{\bullet}S^{*} \underset{k_4}{\overset{k_3}{\rightleftharpoons}} E_{ox}{\bullet}S$$

S = MHPC

(inset of Figure 3), indicative of a mechanism involving a two-step equilibrium process in which an enzyme−substrate complex is initially formed, followed by an isomerization reaction (Strickland et al., 1975) (Scheme 1).

The data were fit to eq 4 by using a Levenberg−Marquardt nonlinear fit algorithm that is included in the KaleidaGraph software. This analysis method gives $k_3 = 48 \pm 1$ s^{-1}, $k_4 = 1.7 \pm 0.7$ s^{-1}, k_2/k_1 (microscopic K_d for primary binding) = 211 ± 16 μM, where k_{obs} = the observed rate.

$$k_{obs} = \frac{k_3[\text{MHPC}]}{[\text{MHPC}] + k_2/k_1} + k_4 \qquad (4)$$

The overall K_d can be calculated by using eq 5 and the above kinetic parameters. A macroscopic K_d of 7.2 μM was obtained from this calculation.

$$K_d = \frac{k_2 k_4}{k_1 k_3}\left(\frac{1}{1 + k_4/k_3}\right) \qquad (5)$$

Equilibrium Binding of MHPC to E_{ox}. The static K_d for binding of MHPC to E_{ox} was also determined by fluorescence and absorbance titrations. The final fluorescence of the E_{ox}−MHPC complex at different concentrations of MHPC (data from Figure 3) was used to calculate the value of K_d for the E_{ox}−MHPC complex (Figure 4). The K_d obtained by this method is 9.2 ± 0.6 μM. The interaction of MHPC with MHPCO also perturbs the absorbance spectrum of the flavin (Kishore & Snell, 1981b), resulting in a decreased absorbance between 450 and 500 nm. Titration of E_{ox} with MHPC monitored by the decrease in absorbance at 490 nm gave a K_d of 9.6 ± 0.7 μM (Figure 4). K_d values from static titrations (9.2 and 9.6 μM) are thus in reasonable agreement

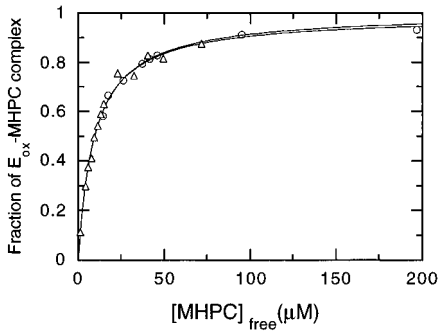

FIGURE 4: Dissociation constant of the MHPCO−MHPC complex. Titrations with MHPC were monitored by fluorescence changes at the completion of binding reactions (Figure 3) (○) or by changes in the absorbance at 490 nm (△). The ordinate is calculated as the fraction of the total change observed. Fits to the data are plotted as smooth lines. Fluorescence data: $K_d = 9.2 \pm 0.6$ μM; absorbance data: $K_d = 9.6 \pm 0.7$ μM.

with the K_d value (7.2 μM) obtained from the kinetic parameters above.

Kinetics of the Binding of 5HN to E_{ox}. The interactions between E_{ox} and 5HN were also studied by stopped-flow fluorimetry, as described above for the binding of MHPC to E_{ox}. The binding of 5HN to the enzyme results in an increase of flavin fluorescence (data not shown) similar to that caused by binding of MHPC to E_{ox}. The rate of this fluorescence increase also shows saturation kinetics, again indicating a two step binding process (Scheme 1).

The same method for analyzing the binding of MHPC to E_{ox} yielded $k_3 = 39 \pm 4$ s^{-1}, $k_4 = 25 \pm 5$ s^{-1}, and $k_2/k_1 = 11 \pm 4$ μM for binding of 5HN. These kinetic constants give an overall K_d value of 4.1 μM. This result was supported by static titration of E_{ox} and 5HN. The final fluorescence of the E_{ox}−5HN complex at different concentrations of 5HN permitted calculation of $K_d = 5.2 \pm 0.4$ μM, which is in reasonable agreement with the K_d of 4.1 μM derived from the kinetic data.

The Binding of Substrate to E_{red}. Since we know the binding constant of substrates to MHPC and the redox potentials of the free enzyme and of the MHPCO−substrate complex, we can use eq 6 (Clark, 1960; Einarsdottir et al., 1988) to calculate the binding constants of substrates to the reduced enzyme.

$$E^{\circ}_{\text{bound}} = E^{\circ}_{\text{m}} - (0.056/n)\log(K_{a,ox}/K_{a,red}) \qquad (6)$$

E°_{bound} = the midpoint potential of the MHPCO−substrate complex; E_m = the midpoint potential of the uncomplexed MHPCO; n = the number of electrons involved; $K_{a,ox}$ = the association constant for substrate and oxidized enzyme; and $K_{a,red}$ = the association constant for substrate and reduced enzyme.

The values of K_d for binding of MHPC and 5HN to the reduced enzyme were calculated to be 7.0 and 4.3 μM, respectively. The kinetic mechanisms and rate constants for the binding of MHPC and 5HN are summarized in Scheme 2 and Table 3. Simulation of the data by numerical methods using this model and kinetic parameters determined above agrees very well with the experimental data (Figure 3).

Reduction of E_{ox}. The reaction between substrate-free MHPCO and NADH was monitored spectrophotometrically under anaerobic conditions in the stopped-flow apparatus. Reduction of the enzyme-bound FAD was very slow, and

Table 3: Rate Constants of Binding of Substrates to MHPCO

substrate	k_1[a] (M^{-1} s^{-1})	k_2[a] (s^{-1})	k_3 (s^{-1})	k_4 (s^{-1})	$K_{d,ox}$ (μM)	$K_{d,red}$ (μM)
MHPC	1.5×10^6	270	48 ± 1	1.7 ± 0.7	9.2 ± 0.6	7.0
5HN	1.5×10^7	200	39 ± 4	25 ± 5	5.2 ± 0.4	4.3

[a] k_1 and k_2 were obtained from data simulation.

Scheme 2

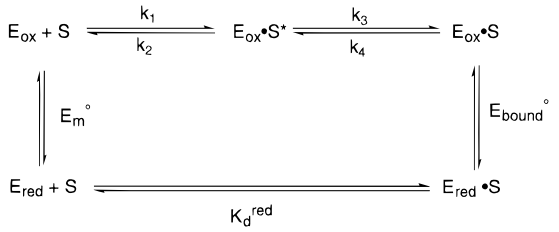

the reaction monitored at 450 nm was monophasic and pseudo-first-order at all concentrations of NADH employed. No transient absorbance changes above 530 nm indicative of flavin semiquinones or charge-transfer complexes were observed. A second-order rate constant of 4.1 ± 0.1 M^{-1} s^{-1} was determined from a linear plot of the apparent rate of reduction versus NADH concentration. A small *y*-axis intercept in this plot indicates some reversibility in the reaction with a reverse rate constant estimated to be 4.1 ($\pm$ 0.5) $\times$ 10^{-4} s^{-1}.

Reduction of the E_{ox}−MHPC and the E_{ox}−5HN Complexes. Reduction of MHPCO by NADH is markedly stimulated by the presence of the substrate MHPC (Sparrow et al., 1969) or by the substrate analog 5HN. The kinetics for the reduction of the E_{ox}−MHPC and E_{ox}−5HN complexes by NADH were examined by fluorescence and absorbance stopped-flow spectrophotometry under anaerobic conditions (Figure 5). No transient long-wavelength absorbing species were observed during the reduction of the enzyme. Therefore, the kinetic data do not indicate the existence of either flavin semiquinones or pyridine nucleotide−enzyme charge-transfer complexes during the reduction.

In stopped-flow absorbance studies, reduction monitored at 450 nm shows an initial lag period followed by the hydride transfer phase, which has a large change in absorbance (trace 2 of Figure 5). At high concentrations of substrate, the observed rate of the hydride transfer phase approached a limit value of 12.7 ± 0.3 s^{-1} for MHPC and 10.0 ± 0.1 s^{-1} for 5HN as substrates (Figure 6). This implies that there is at least a one-step binding process prior to reduction of the E_{ox}−substrate−NADH complex.

In stopped-flow fluorescence studies, the reduction of the E_{ox}−substrate complexes by NADH or NADD results in four phases (traces 4 and 5 of Figure 5), implying that more than one type of E_{ox}−substrate−NADH(D) complex was formed prior to the reduction step. The first phase is a quenching of the enzyme-bound FAD fluorescence during the dead time of the stopped-flow instrument (2 ms) and was observed in both E_{ox}−MHPC (Figure 5) and E_{ox}−5HN (data not shown) reduction. The second phase is a fast but measurable decrease in fluorescence and the apparent rate constant with MHPC bound depends on pyridine nucleotide concentration (Figure 7A). These two phases may represent pyridine nucleotide binding and an ensuing isomerization process.

The third phase of the reductive half reaction results in a fluorescence increase. The amplitude of the fluorescence

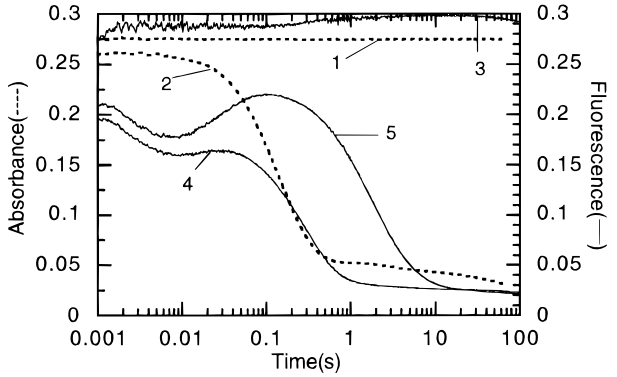

FIGURE 5: Kinetic traces of the reduction of the MHPCO−MHPC complex with NADH(D). (Dotted lines) the reduction of 21.9 μM enzyme by NADH was observed by absorbance at 450 nm: 1, NADH = 0 μM and 2, NADH = 198.8 μM (concentration after mixing). (Solid lines) the reduction of 9.5 μM enzyme by NADH and NADD was monitored by the fluorescence of the flavin with the excitation wavelength of 468 nm and emission wavelengths greater than 515 nm: 3, NADH(D) = 0 μM; 4, NADH = 63.2 μM; 5, NADD = 52.1 μM (concentration after mixing). All experiments were performed in 250 μM MHPC, 50 mM sodium phosphate buffer, pH 7.0, 1 mM DTT, at 4 °C.

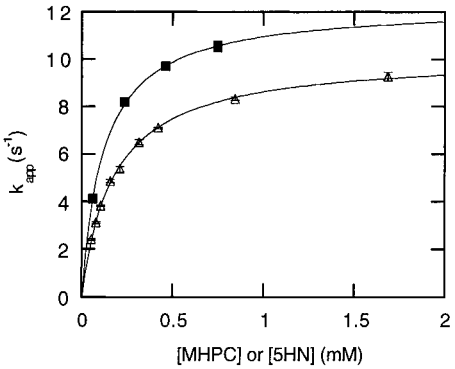

FIGURE 6: Plot of apparent rates of reduction (k_{app}) versus substrate concentration. The k_{app} of the second phase in absorbance stopped-flow experiments (see Figure 5 trace 2) is plotted as a function of MHPC (■) and 5HN (△). At high concentrations of MHPC and 5HN, the k_{app} approached the values of 12.7 ± 0.3 and 10.0 ± 0.1 s^{-1}, respectively.

increase is more pronounced when the enzyme was reacted with NADD than with NADH, because the rate of the subsequent step, the hydride transfer, decreased when NADD was used instead of NADH. One possible model to explain these results is that the third phase may represent a second isomerization of the enzyme−substrate−NADH(D) complexes as in Scheme 3.

However, the inverse dependence of the rates of the third phase on NADH(D) concentration (Figure 7B) is inconsistent with the model in Scheme 3. It is possible that this phenomenon may be attributed to a mechanism in which both forms of E_{ox}−substrate complex (Scheme 1 and 2) can bind NADH(D), but only one form can proceed to reduction, as in Scheme 4. Data simulated according to this model show a reverse dependence on NADD concentration for this phase, consistent with the experimental data.

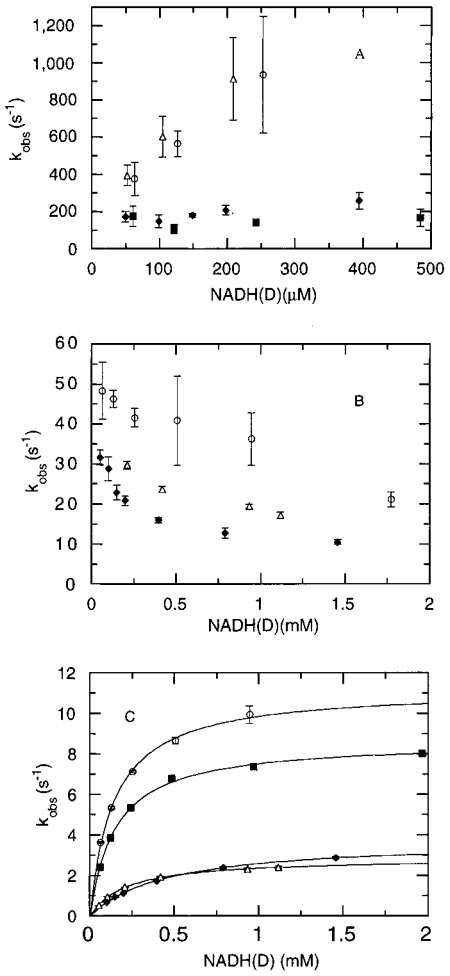

FIGURE 7: Plot of k_{obs} of the reduction of the MHPCO−substrate complex monitored by fluorescence (see traces 4 and 5 Figure 4) as a function of NADH(D) concentration: (○) E_{ox}−MHPC and NADH, (△) E_{ox}−MHPC and NADD, (■) E_{ox}−5HN and NADH, (◆) E_{ox}−5HN and NADD. (A) The observed rates of the fluorescence decrease in the second phase. (B) The rate of the fluorescence increase in the third phase. Note that the observed rates of this third phase for the reduction of E_{ox}−5HN and NADH cannot be precisely determined and are not included since a minimal fluorescence increase was observed in this reaction. (C) The rates of the hydride transfer phase, the fourth phase of the reduction of the enzyme−substrate complex.

Scheme 3

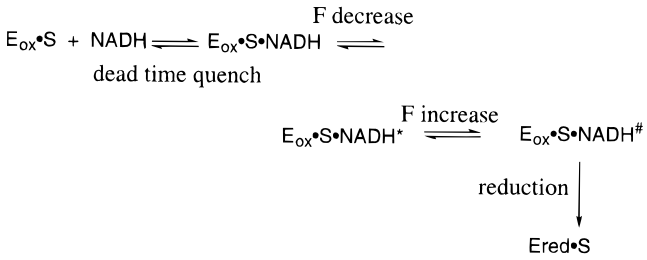

The fourth phase of the reductive half reaction results in a large decrease in fluorescence. This phase represents the hydride transfer step as confirmed by the rate decrease of about 4-fold in the case of the E_{ox}−MHPC complex and about 3-fold for the E_{ox}−5HN complex when NADD was used instead of NADH (Figure 7C). At high concentrations of NADH, the rates of hydride transfer approach a value of 10.7 ± 0.2 s^{-1} for the E_{ox}−MHPC and 8.9 ± 0.1 s^{-1} for the E_{ox}−5HN complexes, respectively. These results agree reasonably with the k_{red} values obtained by absorbance studies, 12.7 ± 0.3 and 10.0 ± 0.1 s^{-1}, respectively.

Scheme 4

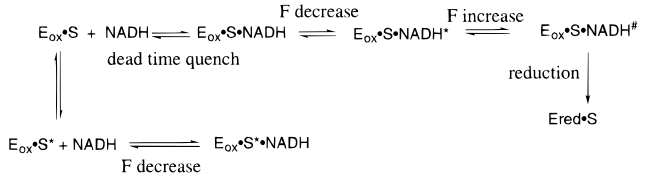

DISCUSSION

The kinetic investigation of the reduction of MHPCO by pyridine nucleotides demonstrates the significant role of the substrate in stimulating the reduction process. Kinetic investigations of the binding of MHPC and of 5HN to the enzyme show that each occurs via a two-step equilibrium reaction in which an MHPCO−substrate complex initially formed is followed by a ligand-induced isomerization of the initial MHPCO−substrate complex (Scheme 1).

A general feature of FAD-dependent monooxygenases is that the aromatic substrate dramatically enhances the rate of reduction of the flavin (Massey & Hemmerich, 1975; Ballou, 1982). *p*-Hydroxybenzoate hydroxylase is the only aromatic flavoprotein monooxygenase whose three-dimensional structure has been elucidated by X-ray crystallography (Van der Lann, 1986; Schreuder et al., 1988, 1990). Although only small differences in conformation were noted when the structure of the uncomplexed enzyme was compared to that of the enzyme−*p*-hydroxybenzoate complex, it was speculated that a conformational change associated with substrate binding might nevertheless be required for rapid reduction of the enzyme by pyridine nucleotide (Van der Lann, 1986). It could likewise be envisioned that the binding of MHPC or 5HN to MHPCO stabilizes a protein conformation necessary for rapid reduction of the enzyme.

The investigation of the redox potentials of the MHPCO and the MHPCO−substrate complexes revealed that the rate enhancement of flavin reduction by pyridine nucleotide upon substrate binding cannot be attributed to the change in redox potentials. All redox potential values of MHPCO, MHPCO−MHPC, and MHPCO−5HN are the same within experimental uncertainty. This indicates that substrate binding exerts its effects by optimizing the relative orientation of the enzyme-bound FAD for effective electron transfer from NADH.

The reduction of the E_{ox}−MHPC and E_{ox}−5HN complexes by NADH(D) studied by stopped-flow fluorimetry revealed a complex mechanism, while the studies by absorbance stopped-flow revealed only an initial lag followed by the hydride transfer phase. The inverse dependence on NADH(D) concentration of the rate of the fluorescence increase during the third phase is inconsistent with the mechanism of Scheme 3. The model in Scheme 4, which assumes that there are two forms of the enzyme−substrate complex at equilibrium that can bind NADH(D), but only one can undergo reduction, seems to be more favored, since simulated data for this model show a reverse dependence on NADH(D) concentration of the rate of the fluorescence increase in the third phase. However, our results are not definitive enough to conclude that the model in Scheme 4 is the kinetic mechanism for the enzyme reduction, nor is it possible to exclude a variety of

other models. It is even conceivable that MHPCO may have a second, regulatory binding site for NADH(D), but the data here are not sufficient to support or refute this model.

MHPCO forms flavin semiquinone intermediate species, either upon reduction with one-electron donors such as the xanthine−xanthine oxidase reduction system, dithionite, or by photoreduction in the presence of 5-deazaflavin. In the absence of MHPC or 5HN, the enzyme stabilizes the anionic flavin semiquinone species (Figure 1A), whereas in the presence of MHPC or 5HN, the neutral flavin semiquinone is stabilized (Figure 1B). When NADH is used as a reductant, no flavin semiquinone can be detected in the reduction. The enzyme salicylate hydroxylase also forms an anionic flavin semiquinone in the absence of effectors and a neutral semiquinone when in complex with salicylate (Einarsdottir et al., 1988; White-Stevens et al., 1972). These observations indicate that in the presence of substrate, formation of the flavin semiquinone involves the transfer of both an electron and a proton (Einarsdottir et al., 1988). The negative charge of substrate at the active site may cause the enzyme−substrate complexes to stabilize the formation of the neutral flavin semiquinone instead of the anionic flavin semiquinone, thereby minimizing the accumulation of negative charge in the active site.

The observation of thermodynamically stable flavin semiquinones in yields of 13−34% by MHPCO contrasts with many of the aromatic FAD-dependent monooxygenases (Massey & Hemmerich, 1978). With *p*-hydroxybenzoate hydroxylase and phenol hydroxylase, a blue neutral flavin semiquinone species could only be detected in anaerobic reductive titrations in the presence of fluorinated substrates (Husain et al., 1980) and chloride anion (Detmer & Massey, 1984). In similar titrations with anthranilate hydroxylase (Einarsdottir et al., 1989) and melilotate hydroxylase (Strickland & Massey, 1973a) no flavin semiquinone accumulates either in the absence or in the presence of substrates. 3-Hydroxybenzoate-6-hydroxylase stabilizes a neutral flavin semiquinone either in the absence or in tje presence of *m*-hydroxybenzoate (Yu et al., 1987). In contrast to aromatic flavoprotein hydroxylases such as *p*-hydroxybenzoate hydroxylase (Howell et al., 1972), melilotate hydroxylase (Strickland & Massey, 1973b; Schopfer & Massey, 1979), and phenol hydroxylase (Detmer & Massey, 1984), which form charge-transfer complexes between FAD enzyme and pyridine nucleotides, no such species were detected during the reduction of MHPCO.

In conclusion, reduction of MHPCO is very similar to that for other aromatic flavoprotein monooxygenases (Massey & Hemmerich, 1975; Howell et al., 1972; Husain & Massey, 1979; Detmer & Massey, 1984; Strickland & Massey, 1973a; White-Stevens & Kamin, 1972; Wang & Tu, 1984; Ohta at al., 1975; Powlowski, et al., 1989a,b; Schopfer & Massey, 1979). The stimulatory effect exerted by the aromatic substrate on the rate of enzyme reduction by pyridine nucleotides is a central feature among aromatic flavoprotein monooxygenases (Massey & Hemmerich, 1975; Ballou, 1982) and has been demonstrated for *p*-hydroxybenzoate hydroxylase (Howell et al., 1972; Husain & Massey, 1979), melilotate hydroxylase (Strickland & Massey, 1973b; Schopfer & Massey, 1979), phenol hydroxylase (Detmer & Massey, 1984), anthranilate hydroxylase (Powlowski et al., 1989a,b; Powlowski et al., 1987), salicylate hydroxylase (White-Stevens & Kamin, 1972; Wang & Tu, 1984), orcinol hydroxylase (Ohta at al., 1975), and p-hydroxyphenylacetate hydroxylase (Arunachalam et al., 1994).

ACKNOWLEDGMENT

We thank Mr. Kevin Kim and Dr. Bruce A. Palfey for the preliminary work on the synthesis of MHPC and Dr. Yerramilli Murthy for recording NMR spectra during the synthesis of MHPC.

REFERENCES

Arunachalam, U., Massey, V., & Miller, S. M. (1994) *J. Biol. Chem. 269*, 150−155.
Ballou, D. P. (1982) in *Flavins and Flavoproteins* (Massey, V., & Williams, C. H., Eds.) pp 301−310, Elsevier, Amsterdam.
Bull, C., & Ballou, D. P. (1981) *J. Biol. Chem. 256*, 12673−12680.
Burg, R. W., Rodwell, V. W., & Snell, E. E. (1960) *J. Biol. Chem. 235*, 1164−1169.
Chaiyen, P., Ballou, D. P., & Massey, V. (1996) 2-Methyl-3-hydroxypyridine-5-carboxylic acid (MHPC) Oxygenase: The Hydroxylase Capable of Catalyzing a Ring Cleavage Reaction, in *Flavins and Flavoproteins* (Stevenson, K. J., Massey, V., & Williams, C. H., Eds.), in press.
Clark, W. M. (1960) in *Oxidation-Reduction Potentials of Organic Compounds*, p 184, Williams and Wilkins, New York.
Detmer, K., & Massey, V. (1984) *J. Biol. Chem. 259*, 11265−11272.
Einarsdottir, G. H., Stankovich, M. T., & Tu, S.-C. (1988) *Biochemistry 27*, 3277−3285.
Einarsdottir, G. H., Stankovich, M. T., Powlowski, J., Ballou, D. P., & Massey, V. (1989) *Biochemistry 28*, 4161−4168.
Entsch, B., & Van Berkel, W. J. H. (1995) *FASEB J. 9*, 476−483.
Gassner, G. T., Wang L., Batie C., & Ballou, D. P. (1994) *Biochemistry 33*, 12184−12193.
Guirard, B. B., & Snell, E. E. (1971) *J. Bacteriol. 108*, 1318−1321.
Hayaishi, O., Nozaki, M., & Abbott, M. T. (1975) in *The Enzymes*, 3rd ed. (Boyer, P. D., Ed.) Vol. 12, Part B, pp 119−189, Academic Press, New York.
Horecker, B. L., & Kornberg, A. (1948) *J. Biol. Chem. 175*, 385−390.
Howell, L. G., Spector, T., & Massey, V. (1972) *J. Biol. Chem. 247*, 4340−4350.
Husain, M., & Massey, V. (1979) *J. Biol. Chem. 254*, 6657−6666.
Husain, M., Entsch, B., Ballou, D. P., Massey, V., & Chapman, P. J. (1980) *J. Biol. Chem. 255*, 4189−4197.
Kishore, G. M., & Snell, E. E. (1979) *Biochem. Biophys. Res. Commun. 87*, 518−523.
Kishore, G. M., & Snell, E. E. (1981a) *J. Biol. Chem. 256*, 4228−4233.
Kishore, G. M., & Snell, E. E. (1981b) *J. Biol. Chem. 256*, 4234−4240.
Kishore, G. M., & Snell, E. E. (1981c) in *Oxygen and Oxy-Radicals in Chemistry and Biology* (Rodgers, M. A. J., & Powers, E. L., Eds.) pp 521−534, Academic Press, New York.
Loesche, W., Wenz, I., Till, U., Petermann, H., & Horn, A. (1980) *Methods Enzymol. 66*, 11−23.
Massey, V. (1991) in *Flavins and Flavoproteins* (Curti, B., Ronchi, S., & Zannetti, G., Eds.) pp 59−66, Walter de Gruyter & Co., Berlin.
Massey, V., & Palmer, G. (1966) *Biochemistry 5*, 3181−3189.
Massey, V., & Hemmerich, P. (1975) in *The Enzymes*, 3rd ed. (Boyer, P. D., Ed.) Vol. 12, Part B, pp 191−252, Academic Press, New York.
Massey, V., & Hemmerich, P. (1978) *Biochemistry 17*, 9−17.
Massey, V., Komai, H., Palmer, G., and Elion, G. B. (1970) *J. Biol. Chem. 245*, 2837−2844.
Nozaki, M. (1974) in *Molecular Mechanisms of Oxygen Activation* (Hayaishi, O., Ed.) pp 135−165, Academic Press, New York.
Ohta, Y., Higgins, I. J., & Ribbons, D. W. (1975) *J. Biol. Chem. 250*, 3814−3825.
Palm, D., Smucker, A. A., & Snell, E. E. (1967) *J. Org. Chem. 32*, 826−828.

Powlowski, J. B., Dagley, S., Massey, V., & Ballou, D. P. (1987) *J. Biol. Chem. 262*, 69−75.
Powlowski, J., Massey, V., & Ballou, D. P. (1989a) *J. Biol. Chem. 264*, 5606−5612.
Powlowski, J., Ballou, D., & Massey, V. (1989b) *J. Biol. Chem. 264*, 16008−16016.
Press, W. H., Teukolsky, S. A., Vetterling, W. T., & Flannery B. P. (1992) in *Numerical Recipes in C, The Art of Scientific Computing*, 2nd ed., pp 683−688, Cambridge University Press, New York, NY.
Schopfer, L. M., & Massey, V. (1979) *J. Biol. Chem. 254*, 10634−10643.
Schreuder, H. A., van der Laan, J. M., Hol, W. G. J., & Drenth, J. (1988) *J. Mol. Biol. 199*, 637−648.
Schreuder, H. A., Hol, W. G. J., & Drenth, J. (1990) *Biochemistry 29*, 3101−3108.
Sparrow, L. G., Ho, P. P. K., Sundaram, T. K., Zach, D., Nyns, E. J., & Snell, E. E. (1969) *J. Biol. Chem. 244*, 2590−2600.
Stiller, E. T., Keresztesy, J. C., & Stevens, J. R. (1939) *J. Am. Chem. Soc. 61*, 1237−1242.
Strickland, S., & Massey, V. (1973a) *J. Biol. Chem. 248*, 2944−2952.
Strickland, S., & Massey, V. (1973b) *J. Biol. Chem. 248*, 2953−2962.
Strickland, S., Palmer, G., & Massey, V. (1975) *J. Biol. Chem. 250*, 4048−4052.
Sundaram, T. K., & Snell E. E. (1969) *J. Biol. Chem. 244*, 2577−2585.
Van der Laan, J. M. (1986) On the Enzymatic Cycle of *p*-Hydroxybenzoate Hydroxylase: An X-Ray Diffraction Study, Ph.D. Thesis, University of Groningen, The Netherlands.
Wang, L.-H., & Tu, S.-C. (1984) *J. Biol. Chem. 259*, 10682−10688.
White-Stevens, R. H., & Kamin, H. (1972) *J. Biol. Chem. 247*, 2358−2370.
White-Stevens, R. H., Kamin, H., & Gibson, Q. H. (1972) *J. Biol. Chem. 247*, 2371−2381.
Yu, Y., Wang, L.-H., & Tu, S.-C. (1987) *Biochemistry 26*, 1105−1110.

BI962325R